

Insulator-metal transition in high- T_c superconductors as result of percolation over -U centers

K. V. Mitsen and O. M. Ivanenko

Department of Solid State Physics, P. N. Lebedev Physical Institute RAS, Moscow 117924, Russia
(February 1, 2008)

The mechanism of -U center formation in high- T_c superconductors (HTS) with doping is considered. It is shown that the transition of HTS from insulator to metal passes through the particular dopant concentration range where the local transfer of singlet electron pairs from oxygen ions to pairs of neighboring cations (-U centers) are allowed while the single-electron transitions are still forbidden. We believe it is this concentration range that corresponds to the region of high- T_c superconductivity and the interelectron attraction results from the interaction of electron pairs with -U centers. Additional hole carriers are generated as the result of singlet electron pair transitions from oxygen ions to -U-centers. The orbitals of the arising singlet hole pairs are localized in the nearest vicinity of -U center. In such a system the hole conductivity starts up at the dopant concentration exceeding the classical 2D-percolation threshold for singlet hole pair orbitals. In the framework of the proposed model the phase diagram Ln-214 HTS compounds is constructed. The remarkable accord between calculated and experimental phase diagrams may be considered as the confirmation of the supposed model. The main features of hole carriers in HTS normal state are found to be the nondegenerate distribution and the dominant contribution of electron-electron scattering to the hole carrier relaxation processes. Various experimentally observed anomalies of HTS properties are shown to be the consequences of the above-mentioned features. The conclusion is made that HTS compounds are the special class of solids where the unusual mechanism of superconductivity different from BCS is realized.

I. INTRODUCTION

In 13 years elapsed after the discovery of HTS,¹ numerous models have been suggested (see review in Ref. 2) to explain the nature of the ground state and anomalous properties of HTS compounds. However, the lack of any crucial experiment gave no way of choosing between these models.

In this paper, we intend to demonstrate that the mechanism responsible for various anomalous properties of HTS compounds (including the high-temperature superconductivity itself) is apparently based on interaction of electrons with so-called -U centers.³ To this end, we consider the way the insulator-metal transition occurs in HTS under doping. On the basis of a simple ionic model, we will show that such a transition should pass through a certain range of dopant concentrations; this range corresponds to the situation when local transitions of singlet electron pairs from oxygen ions to a pair of neighboring cations (-U center) become possible in individual microclusters including several unit cells, while the single-electron transitions are still forbidden. In our opinion, it is this range of concentrations that corresponds to the HTS range where interelectron attraction results from interaction of electron pairs with -U centers.⁴⁻¹⁰ Conduction in such a system arises when the concentration of -U centers exceeds the percolation threshold for orbitals of singlet hole pairs. We are going to consider which specific fragments of crystal structure are involved

in the formation of -U centers and what is the range of existence of infinite percolation cluster interconnecting singlet hole pair orbitals. On this basis we will construct the phase diagram for Ln-214 (Ln=La, Nd) compounds. In our opinion, a comparison of this phase diagram with the carefully investigated diagram for Ln-214 compound should be taken as the aforementioned crucial experiment for choosing the mechanism responsible for the HTS properties. We discuss the special features of phase diagrams for Ln-214 with n - and p -type of doping, and also we give a somewhat different interpretation of some experimental results obtained for underdoped HTS. Furthermore, we consider the nature of mobile hole carriers and mechanism of their relaxation in HTS. As will be seen the distinctive feature of HTS normal state is the nondegenerate distribution of hole carriers that results in hole-hole scattering to dominate in kinetic processes. It will be shown that this feature may account for the unusual transport and optical properties of HTS observed in experiment.

II. -U CENTER FORMATION IN HTS

There are good reasons to believe that electronic spectrum of insulator phase for various HTS compounds in the vicinity of Fermi energy E_F can be best approximated by the model of charge-transfer insulator.¹¹ In this model, the upper empty band formed by unfilled orbitals of cations is separated with a gap from the O2p band

formed largely by oxygen states (Fig. 1(a)). The gap Δ_{ct} existing in the spectrum is related to the transfer of electron from oxygen to the neighboring cation and lies in the range of 1.5 – 2 eV for all HTS.¹²

The question arises: What is the mechanism of insulator-metal transition in the doped HTS? As an example of HTS, we consider Ln-214. For these compounds, the quantity Δ_{ct} , in terms of simple ionic model, is defined by the following relationship:¹³

$$\Delta_{ct} \approx |\Delta E_M| + A_p - I_d. \quad (1)$$

Here, I_d is the second ionization potential of Cu, A_p is the electronegativity of oxygen with respect to formation of O^{2-} , and $|\Delta E_M|$ is the difference of the Madelung energy E_M between the configuration in which the copper and oxygen atoms are in the state of Cu^{2+} and O^{2-} and that with these atoms in the states of Cu^{1+} and O^{1-} . Taking into account¹⁴ that $I_d \sim 20$ eV, $A_p \sim 0$ eV and $\Delta_{ct} \sim 1.5 - 2$ eV, there is a subtle balance between these three quantities.

This balance can be varied by heterovalent doping; for example by doping the La_2CuO_4 with divalent Sr or by doping Nd_2CuO_4 with tetravalent Ce. It is a matter of great importance that the charge carriers introduced by doping (so-called doped carriers) are localized¹⁵⁻¹⁷ (at least for low concentrations) in CuO_2 plane in the vicinity of the dopant ion: either at the $O2p_{x,y}$ orbitals (the holes in $La_{2-x}Sr_xCuO_4$) or at the $Cu3d_{x^2-y^2}$ orbitals (electrons in $Nd_{2-x}Ce_xCuO_4$). Taking into account that the interaction of O^{2-} and Cu^{2+} gives the main contribution to E_M , an addition both of electrons (to the Cu orbitals) and of holes (to the oxygen orbitals) will result in the same thing: a decrease in $|\Delta E_M|$ and, correspondingly, a decrease in Δ_{ct} for other pairs of copper and oxygen ions sited in the vicinity of the doped carrier. For a certain critical concentration x_c , the gap Δ_{ct} vanishes throughout the entire crystal. As a result, electron transitions from oxygen to copper become possible, and the material passes into a normal metal.

In generally by this means, we can conceive the transition of a charge-transfer insulator into the metallic state with doping in terms of ionic model. However, we argue that, in HTS compounds, the transition from insulator to metal with x passes through a special range of concentrations $x_0 < x < x_c$ for which the two-electron transitions from oxygen ions to certain pairs of neighboring cations become possible, while the single-electron transitions are still forbidden. In other words, -U centers are formed on certain pairs of cations at $x_0 < x < x_c$.

Let us consider a $Cu_2M_2O_n$ cluster where two neighboring Cu ions belong to the CuO_2 plane, and $M=Cu$ in the selfsame CuO_2 plane for Ln-214, $M=Cu$ in the CuO_3 chain for $YBa_2Cu_3O_7$, and $M=Bi$ for $Bi_2Sr_2Ca_2Cu_2O_{8+\delta}$. As will be seen from the following consideration, the condition for the formation of -U centers at the neighboring Cu ions in CuO_2 plane consists in the presence of one doped carrier in the vicinity of each M

ion (in $YBa_2Cu_3O_7$ and $Bi_2Sr_2Ca_2Cu_2O_{8+\delta}$, these carriers are in the CuO_3 chains and BiO planes, respectively). In Ln-214, two types of such clusters are possible (Figures 2(a, b)): the projections of the dopant ions onto the CuO_2 plane are separated by either $3a$ or $a\sqrt{5}$, where a is the lattice constant in the CuO_2 plane. In both cases, the presence of doped carrier in the vicinity of each M ion reduces Δ_{ct} for the neighboring Cu ions and, as it will be shown, provides the conditions (i.e., forms a local minimum of potential energy) for simultaneous transition of two electrons to the pair of interior Cu ions from O ions surrounding this pair. It should be noted here that, in the intermediate case where the M ion projections are spaced $a\sqrt{8}$ apart, such pair of Cu ions does not emerge (Fig. 2(c)).

It is possible to estimate a decrease in Δ_{ct} for a given Cu ion in La-214 due to the presence of a single hole around the neighboring Cu ion if we assume that this hole is "distributed" (Fig. 3) over 12 nearest-neighbor oxygen ions (the first and second coordination spheres). This assumption is consistent with experimentally determined limit of substitutability (see below). We take into account only the interaction between the nearest neighbors. Therefore we consider 3 oxygen ions from the total number of 12, where the hole "feels" the unscreened Cu ion separated by a distance of $r = a/2 \approx 2$ Å from this hole. In this case for a given Cu ion, a lowering of the $Cu3d^{10}$ state energy amounts to $\Delta E \sim (1/4)e^2/r \sim 1.8$ eV; here, e is the electron charge. This means that, due to doping, the $Cu3d^{10}$ state energy for a given Cu ion is decreased, so that it is now by $\Delta E \sim 1.8$ eV below the bottom of the conduction band for undoped material. This value is still smaller by $\sim 0.1 - 0.2$ eV than $\Delta_{ct} \approx 1.9 - 2.0$ eV for La_2CuO_4 .¹² In Nd-214 doped electrons increase O2p state energy around M ion that results in a decrease in Δ_{ct} , too.

An additional lowering of the $Cu3d^{10}$ state energy is attained owing to formation of a bound state of two electrons at neighboring Cu ions in the presence of two holes in the immediate vicinity of this pair. Such a decrease is possible for a bonding orbital of a singlet hole pair, as is the case for H_2 molecule. Here, this analogy is even more appropriate because the distance between electrons at Cu ions (≈ 3.8 Å) is close to $R_0\epsilon_\infty \approx 3.6$ Å, where $\epsilon_\infty \approx 4.5$ is the high-frequency dielectric constant¹⁸ and $R_0 \approx 0.8$ Å is the distance between nuclei in H_2 molecule. Therefore, an additional lowering of the energy δE_U due to transition of two electrons to neighboring copper ions can be, in the case under consideration, estimated from the relationship $\delta E_U \sim \delta E_H/\epsilon_\infty^2 \approx 0.23$ eV, where $\delta E_H = 4.75$ eV is the binding energy in H_2 molecule. However, this value δE_U is apparently underestimated because oxygen ions in CuO_2 plane efficiently screen the repulsive interaction of electrons at Cu ions and weakly screen the electron-hole attraction.

Thus, we may assume that Δ_{ct} , which amounts to 1.5 – 2.0 eV for doped cuprates,¹² vanishes for two-

electron transitions to neighboring Cu ions. In this case, holes apparently occupy predominantly $\pi p_{x,y}$ orbitals, thus providing naturally the bonding character of the hole-pair orbital owing to configuration of bonds in the CuO_2 plane, which allows the holes to reside in the space between Cu ions (Fig. 4). Here we assume that the states at the top of the oxygen valence band are formed predominantly by $\pi p_{x,y}$ orbitals.¹⁹

It follows from the above consideration that, if an appropriate local minimum in Δ_{ct} is formed, the bound electron state can arise at the pair of neighboring Cu ions while the single-electron transitions are forbidden (i.e., -U center is formed).²⁰ In this case, a singlet hole pair is localized in the vicinity of -U center at a distance of $\sim a/2$. The region of the hole-pair localization is restricted by the condition that the pair level lies in line with the top of the valence band (the energy of the pair level becomes higher with increasing of the hole-pair localization area). Thus, the energy spectrum of CT-insulator under doping is modified by the addition of electron pair level lying in line with the top of the valence band (Fig. 1(b)). In this case the states at the top of valence band should be consider as formed by the $\pi p_{x,y}$ orbitals of oxygen ions surrounding -U centers.

Conduction in such a system occurs if the areas of the localization of singlet hole pairs form a percolation cluster. The localization areas of doped holes may enter into this percolation cluster, too (e.g. in La_{2-14}). The percolation threshold for the hole-pair orbitals of the -U centers in Ln-214 is coincident with that for a ensemble of segments of length $L = 3a$ or $a\sqrt{5}$ in square lattice. The region of delocalization of hole carriers in the percolation cluster is also restricted by the condition that the position of the pair level should coincide with the valence-band top. Such a mechanism keeps the pair level exactly at the top of the valence band (Fig. 1(b)).

On the other hand, if projections of two M ions are separated by a distance $2a$ (Fig. 2(d)), Δ_{ct} vanishes for single-electron transitions to interior Cu ion as well.²¹ Such a fragment is a nucleus of ordinary metallic phase. For the relevant concentrations $x \geq x_c$, the entire crystal transforms into ordinary metal. This state corresponds to a single-band electron spectrum. In $\text{La}_{2-x}\text{Sr}_x\text{CuO}_4$ in the ordinary metal phase, the charge carriers are electrons because, due to doping with divalent Sr, the filling of the band $\rho < 1/2$; under the same conditions, the charge carriers are holes in $\text{Nd}_{2-x}\text{Ce}_x\text{CuO}_4$ because, due to doping with tetravalent Ce, we have $\rho > 1/2$. The intermediate range of x where -U centers and ordinary metal phase are coexisted in the percolation cluster is so-called "overdoped" region. In this case, the additional carriers from metal phase decrease $|\Delta E_M|$ and lower the pair level below the top of the valence band.

III. CONSTRUCTION OF PHASE DIAGRAM OF Ln-214 COMPOUNDS

We will construct the phase diagram for Ln-214 system using the following assumptions:

- (i) the -U centers are formed at the pairs of neighboring Cu ions belonging only to the clusters with $L = 3a$ and $L = a\sqrt{5}$;
- (ii) the orbitals of hole pairs are in the immediate vicinity of these pairs at a distance of $a/2$;
- (iii) conduction in the system arises in the case of percolation over segments containing -U centers; and
- (iv) localized doping carriers cannot be separated by a distance smaller than $2a$.

Assumption (iv) follows from the existence of the substitutability limits in Ln-214 $x_{lim} \approx 0.2 - 0.25$.²²⁻²⁴ If these limits are exceeded, a decomposition of single-phase state and/or a change of the oxygen content occur. In our opinion, the existence of the substitutability limit is related to repulsive interaction between localized doped carriers. In turn, such a repulsion would affect the dopant ion distribution, if the mobility of these ions at heat treatment temperature was rather high. Therefore, we believe that the dopant ions (more precisely, their projections onto the CuO_2 plane) cannot be separated by a distance $L < 2a$ as well.

Taking into account the above assumption, we may define the 2D-percolation threshold as follows. Let us assume that we have a square lattice with the cell parameter $a=1$ and let a fraction x of the sites be occupied by atoms. In order to determine the percolation threshold for segments with length L (i.e., for the pairs of atoms separated by a distance L) we locate each occupied site at the center of circle with the radius $L/2$ (Fig. 5(a)). The sum of the areas of the circles constructed around these atoms is given by $S = \pi x L^2/4$. For a square lattice, the percolation sets in when $S \geq 0.466$.²⁵ Consequently, the concentration corresponding to the percolation threshold is given by $x_p(L) = 0.593/L^2$. Here, we assume that the distribution of atoms over the sites is random, and L is the smallest distance between atoms for the given concentration. Otherwise, we would have an overlapping of circles (Fig. 5(b)), and the value of x_p would be larger than that obtained from the above relationship. In this case a percolation cluster would include not only the segments with a length of L but also those with smaller length (linking the sites separated by smaller distances). The maximal number of segments with length $L - x_M(L)$ - can be attained in the case of ordered arrangement of atoms in a square lattice with the parameter L ; i.e., $x_M(L) = 1/L^2$. The values of x_p and x_M for various values of L are listed in Table 1. Therein, in the righthand column, it is indicated which state (insulator, metal, or HTS) would correspond to the case of percolation over the segments with a given L .

Figure 6(a) shows the percolation ranges for segments with different length L (therein, the corresponding value

of L^2 is indicated to left of each rectangle). The left side of each rectangle corresponds to the $2D$ -percolation threshold for the segments with the length L under the condition that the atoms are randomly distributed and there are no segments with the length smaller than L . The right side of each rectangle corresponds to the point x_M . Heavy lines indicate the percolation ranges for the segments with $L = 3$ and $L = \sqrt{5}$. It is in these concentration regions we suggest, the high-temperature superconductivity occurs.

As will be evident from what follows, the ratio between order and disorder in the distribution of dopants over the sites is very important and defines all special features of phase diagrams for HTS of Ln-214 type. We believe that a tendency towards ordering is related to the difference in ionic radii of Ln and the dopant. This tendency should be most pronounced for the La/Ba pair and least pronounced for the Nd/Ce pair. The degree of ordering should also increase with increasing x (with decreasing L). In what follows, while on subject of the dopant ordering, we imply a formation of a large number of ordered clusters (with sizes smaller than 100 Å) separated by thin walls with random distribution of the dopant. In these walls, the constraint $L \geq 2$ is also preserved. Thus, only the short-range order exists in the system. It is assumed that, if the value of x_M is exceeded, a transition to random distribution of atoms over the sites occurs with formation of an infinite percolation cluster with a smaller value of L .

We now consider various ranges of concentrations in Fig. 6(a) assuming that, at each point $x > 0.1$, no more than two types of segments exist.

1. $0.20 < x < 0.25$. In this case, the $2D$ -percolation is effected over the segments with $L = 2$, i.e., over the clusters of ordinary metal.

2. $0.148 < x < 0.20$. In this range, the $2D$ -percolation threshold for the segments with $L = 2$ depends on the degree of ordering of the dopant atoms with $L = \sqrt{5}$. In the case of ordering of the atoms with $L = \sqrt{5}$, percolation over the segments with $L = 2$ sets in at $x = 0.2$, whereas, for random distribution, percolation over the segments with $L = 2$ is attained at $x = 0.148$. Therefore, this range of x corresponds either to HTS, or to a mixed state of HTS and ordinary metal.

3. $0.125 < x < 0.148$. Here, we have a "pure" $2D$ -percolation over the segments with $L = \sqrt{5}$. This range corresponds to HTS.

4. $0.118 < x < 0.125$. If the atoms with $L = \sqrt{8}$ are ordered, percolation over the segments with $L = \sqrt{5}$ sets in at $x = 0.125$, whereas, if the atoms with $L = \sqrt{8}$ and $L = \sqrt{5}$ are randomly distributed, percolation over the segments with $L = \sqrt{5}$ sets in at $x = 0.118$. In this range, we have either insulator (in the former case) or HTS (in the latter case).

5. $0.111 < x < 0.118$. This is the domain of "pure" $2D$ -percolation over the segments with $L = \sqrt{8}$. This phase corresponds to an insulator.

6. $0.10 < x < 0.111$. In the case of ordering of atoms

with $L = 3$, the $2D$ -percolation over the segments with $L = 3$ sets in at $x = 0.10$, whereas, if the atom pairs with $L = 3$ and $L = \sqrt{8}$ are randomly distributed, there is no $2D$ -percolation neither over the two types of segments. In this case, a percolation cluster would include the areas with $L=3$ (HTS) and with $L = \sqrt{8}$ (insulator) and the conduction is possible only through the tunneling between clusters with $L = 3$ ($3D$ -percolation).

7. $0.066 < x < 0.10$. In this range, there is no $2D$ -percolation over the segments with $L = 3$. $3D$ -percolation (and superconductivity) is still possible for $x > 0.077$, whereas, for $x < 0.077$, there is no bulk superconductivity.

For comparison, Figures 6(b - d) show the experimental phase diagrams $T_c(x)$ for $\text{La}_{2-x}\text{Ba}_x\text{CuO}_4$,²⁶ $\text{La}_{2-x}\text{Sr}_x\text{CuO}_4$,²⁷ and $\text{Nd}_{2-x}\text{Ce}_x\text{CuO}_4$.²⁸ Comparing Figures 6(a - d), we can readily see that all particular points in experimental phase diagrams practically coincide with the boundaries of percolation domains corresponding to the segments with different values of L . Difference between the phase diagrams of $\text{La}_{2-x}\text{Ba}_x\text{CuO}_4$ and $\text{La}_{2-x}\text{Sr}_x\text{CuO}_4$ consists in the fact that, in the former case, a dip in T_c occurs at $x_d = 0.125$, whereas, in the latter case, it takes place at $x_d = 0.115$. It is reasonable to relate the difference in the values of x_d for these compounds to a larger degree of ordering in the La/Ba sublattice as compared to that for La/Sr, as a result of which the percolation threshold for the segments with $L = \sqrt{5}$ becomes shifted to $x = 0.125$ (the point of the highest ordering for $L = \sqrt{8}$).

The maximum of T_c at $x \approx 0.15$ is related to the fact that the ordinary metal clusters appear within the superconducting phase for $x > 0.148$. Because of this, superconductivity is "depressed" to a degree corresponding to the ratio of the volumes occupied by superconducting and metal (nonsuperconducting) phases. This is confirmed²⁹ by measurements of the Meissner-phase volume as a function of a magnetic field. These measurements show that, for $x = 0.15$, this volume is virtually independent of the field, whereas, for $x > 0.15$, a magnetic field reduces significantly the volume of superconducting phase. At the same time, in low fields, the magnitude of the Meissner effect increases^{22,29} with x up to $x \approx 0.2$, which is indicative of ordering of the dopants with $L = \sqrt{5}$.

In $\text{Nd}_{2-x}\text{Ce}_x\text{CuO}_4$ (Fig. 6(d)), there is virtually no ordering of Ce owing to a small differences in sizes of Nd and Ce ions. Therefore, the $2D$ -percolation is possible only for $x > 0.118$ (for $L = \sqrt{5}$).³⁰ However, due to the absence of ordering, a percolation cluster would also include the regions with $L = 2$; thus, the percolation threshold for $L = \sqrt{5}$ shifts to that for $L = 2$. This is consistent with experimental phase diagram.

The region $x < 0.12$ for $\text{La}_{2-x}\text{Ba}_x\text{CuO}_4$ and $\text{La}_{2-x}\text{Sr}_x\text{CuO}_4$ deserves special consideration (the region of "underdoping"). As it follows from Fig. 6a, even the $3D$ -percolation is not possible for $x < 0.077$, and only the "traces" of superconductivity can be observed.

This conclusion is consistent with the results reported in^{31,32} where the bulk superconductivity was not observed in $\text{La}_{2-x}\text{Sr}_x\text{CuO}_4$ for $x = 0.08$. As mentioned above, it is not to be expected that the 2D-percolation can originate (at least, in $\text{La}_{2-x}\text{Sr}_x\text{CuO}_4$) in the range of $0.08 < x < 0.12$ as well because the percolation regions for three different types of segments with $L^2 = 8, 9$, and 10 are close to each other. Most likely, we can have here a tunneling between clusters with $L = 3$. This inference accounts for the results reported in Ref. 33 where, in $\text{La}_{2-x}\text{Sr}_x\text{CuO}_4$ at $T \rightarrow 0$, a logarithmic divergence of resistivity was observed for $x < 0.15$, with superconductivity being depressed by a magnetic field.

The proposed model allows to give an alternate interpretation of the experiments on the pseudogap observation in under- and optimally-doped HTS.³⁴⁻³⁶ As it follows from experiment the pseudogap has the same symmetry and about the same value as the superconducting gap but it vanishes at $T^* > T_c$ (T^* decrease with x down to T_c).

We believe that the observed pseudogap is nothing but just the same superconducting gap opening at $T > T_c$ because of the large fluctuations of the number of particles between valence band and pair level in the short chains of -U centers. The point is that in HTS the mechanism of the superconducting gap suppression is the occupation of pair level with electrons. Therefore the decrease of pair level occupation by fluctuation may result in turning on superconductivity in such chains at $T^* > T_c$ (first-order phase transition.³⁷) At small x the great bulk of -U centers are grouped on short chains where large relative fluctuations of the number of particles are possible. With x the increasing part of -U centers belong to the infinite percolation cluster. Therefore T^* decrease with x down to T_c , unless all -U centers are integrated in infinite percolation cluster.

Thus, we may conclude that all special features observed in phase diagrams of Ln-214 HTS represent no more than geometric relations in a square lattice and a competition between ordering and disorder in distribution of the dopant ions. These items determine the range of existence of infinite percolation cluster integrating the localized orbitals of singlet hole pairs of -U centers. The agreement between experimental and calculated phase diagrams supports the conclusion that it is the considered fragments involving the pairs of neighboring Cu ions in the CuO_2 plane which are responsible for superconductivity in Ln-214. It is interesting that the percolation cluster in Ln-214 resembles the Little's polymer³⁸ while that in $\text{YBa}_2\text{Cu}_3\text{O}_7$ and $\text{Bi}_2\text{Sr}_2\text{Ca}_2\text{Cu}_2\text{O}_{8+\delta}$ (where doped holes are in the plane parallel to the CuO_2 plane) resembles Ginsburg's sandwich.³⁹

IV. HOLE CARRIER GENERATION AND RELAXATION PROCESSES IN HTS

Now we consider the process of the generation of hole carriers as well as the features of the transport and optical properties of HTS in the framework of the proposed model of electronic spectrum (Fig. 1(b)). Let there is an infinite cluster including a quantity of -U centers together with the nearest oxygen ions. The two-particle hybridization of the pair states with the $\text{O}2p_{x,y}$ states of oxygen ions surrounding -U centers results in the broadening both of the pair states and of the $\text{O}2p_{x,y}$ ones. (In this case the electrons at the top of the valence band resemble the "marginal" Fermi liquid).⁴⁰ The pair level broadening can be expressed^{9,10} as $\Gamma \sim \pi(DV)^2 kT$, where V is the constant of hybridization, D is the density of states at the top of $\text{O}2p$ band. The broadening of band states is $\gamma \sim \Gamma/DE_0$, where E_0 is the energy width of statistic distribution of pair states over sites. This broadening smoothes the features of the band state density and results in its independence on energy over the interaction range. The occupation of pair level results from transitions of electrons from $\pi p_{x,y}$ oxygen orbitals to the -U centers and accompanied by the generation of hole carriers in the oxygen band. We call the phase where the additional hole carriers appear through this mechanism as -U phase. The electron occupancy of -U centers η as well as the hole concentration n in -U phase are determined by the balance of rates of electron pair transitions from oxygen band to pair level and back. If N is -U center concentration so $n = 2N\eta$. The rate of electron transitions from pair level to singlet orbitals is proportional to $N\eta\Gamma \sim \eta T$. The rate of reverse process is determined by the frequency of electron-electron scattering and proportional to $\gamma^2(1 - \eta) \propto T^2(1 - \eta)$. Therefore

$$n = 2NT/(T_0 + T), \quad (2)$$

where T_0 is temperature-independent value. Thus $n \propto T$ at low temperature and tends to $2N$ at high temperature. This is in agreement with the data of Hall measurements in $\text{YBa}_2\text{Cu}_3\text{O}_7$, where doped carriers in chains do not contribute to Hall conductivity.^{41,42} As it follows from the above consideration the hole carrier distribution turns out to be nondegenerated owing to the interaction with -U centers. Taking into account the nondegeneracy of carrier distribution (absence of the Pauli blocking) and their high concentration ($10^{21} - 10^{22} \text{ cm}^{-3}$) the electron-electron scattering (more precisely to say hole-hole scattering in this case) is likely to provide the dominant contribution to the relaxation processes in HTS. As far as the interaction of two holes in the system with -U centers corresponds to the effective attraction, it will not be conventional Coulomb scattering. The main mechanism of carrier relaxation in HTS is likely to be similar to that assumed for the metals and alloys with strong electron-phonon coupling.⁴³ In these materials the electrons in a layer $\sim k\Theta_D$ at the Fermi surface (Θ_D is Debye temperature) are attracted due to

virtual phonon exchange. This electron-electron interaction enhanced by phonon-mediation effects far exceeds the screened Coulomb repulsion. Therefore in the metals with strong electron-phonon interaction the dominant channel of the electron-electron scattering will be determined by the virtual phonon exchange. The contribution of these processes becomes essential⁴³ for $T < \Theta_D$ with the amplitude of the electron-electron scattering being independent of scattering particle energy E for $E \ll k\Theta_D$ and dropping sharply at $E \sim k\Theta_D$. For $E > k\Theta_D$ only the Coulomb interaction gives the contribution to the amplitude of electron-electron scattering. The electron-electron contribution to the electrical resistivity ρ ($\rho = AT^2$) exceeding the electron-phonon one, have been observed experimentally for Al at $T < 4$ K and for the A15 superconductors at $T < 50$ K,^{44,45} with the amplitude A more than one order exceeding the result of calculations based on the Coulomb mechanism of scattering.

The dominant relaxation process in HTS is the electron-electron scattering as well and the main channel of this scattering is the interaction of hole pairs on -U centers. This process may be considered as an exchange by virtual bosons (exitons) with energy W . As far as $W \sim 0.1 - 1$ eV (in contrast to the exchange by virtual phonon with energy $E \sim k\Theta_D < 0.03$ eV) the temperature range, where the scattering processes with exchange of virtual bosons are dominant, expands to $T \sim 10^3$ K. The temperature dependence $\rho(T)$ in such a model may be obtained from the Drude formula $\rho = m^*\nu/ne^2$ (here m^* is the effective mass of holes, ν - the rate of hole-hole scattering). For $W \gg E$ the amplitude of scattering doesn't depend on the particle energy. Assuming that density of states is energy-independent ν will be determined only by the hole concentration and statistical factor in scattering cross-section (i.e. the phase volume available for occupation with scattered particles). The latter is proportional to $E_1 + E_2$ (here E_1 and E_2 are the energies of scattering holes measured from the top of valence band). Thus

$$\nu \propto n(E_1 + E_2). \quad (3)$$

For dc-conductivity $E_1 \sim E_2 \sim \gamma \propto T$ and $\nu \propto nT$, so that $\rho(T) \propto T$. This kind of dependence has been observed experimentally for the optimally doped samples of $\text{YBa}_2\text{Cu}_3\text{O}_7$, $\text{La}_{2-x}\text{Sr}_x\text{CuO}_4$, $\text{Bi}_2\text{Sr}_2\text{Ca}_2\text{Cu}_2\text{O}_{8+\delta}$ and others. The dependence $\rho(T) = \rho_0 + bT$ observed frequently in experiments may be explained by the contribution of insulating tunnel barriers interlayering the areas of the -U phase that results in temperature-independent term r_0 . For the overdoped samples where both -U phase and metal phase coexist the additional carriers from metal phase decrease $|\Delta E_M|$ and lower the pair level δE below the top of the valence band. In this case the distribution of hole carriers degenerates and n is temperature-independent for $\gamma \ll \delta E$. The temperature-dependent contribution in resistivity is $\rho(T) \propto \gamma^2 \propto T^2$.

For $\gamma \gtrsim \delta E$ the transition to the linear dependence $\rho(T)$ takes place.

The dominant contribution of electron-electron scattering into the scattering process also has an effect upon both of frequency and temperature dependencies of optical conductivity σ_{opt} :

$$\sigma_{opt} = \frac{e^2 n}{m^*} \frac{\nu_{opt}}{\omega^2 + \nu_{opt}^2} \quad (4)$$

here ω is the photon frequency, ν_{opt} - the rate of optical relaxation. For the electron-electron scattering (at $n = 10^{21} - 10^{22} \text{ cm}^{-3}$) the collision frequency is $\sim 10^{14} - 10^{15} \text{ s}^{-1}$. Thus $\nu_{opt} \gg \omega$ for IR region and the formula for optical conductivity becomes more simple:

$$\sigma_{opt}(\omega, T) = e^2 n / m^* \nu_{opt}. \quad (5)$$

For optical relaxation we have $E_1 \sim \omega$, $E_2 \sim \gamma \propto T$. From where $\sigma_{opt} \propto \omega^{-1}$ (for $\omega \gg \gamma$) and $\sigma_{opt} \propto T^{-1}$ (for $\omega < \gamma$). These results are in a good agreement with the data of various experiments^{46,47}.

V. CONCLUSIONS

The mechanism of -U center formation in high- T_c superconductors (HTS) with doping is considered. It is shown that the transition of HTS from insulator to metal passes through the particular dopant concentration range where the local transfer of singlet electron pairs from oxygen ions to pairs of neighboring cations (-U centers) are allowed while the single-electron transitions are still forbidden. The additional hole carriers are generated as the result of singlet electron pair transitions from the oxygen ions to the -U-centers. The orbitals of the arising singlet hole pairs are localized in the nearest vicinity of -U center. In such a system the hole conductivity starts up at the dopant concentration exceeding the classical 2d-percolation threshold for singlet hole pair orbitals of -U centers. The main features of hole carriers in HTS normal state are found to be the nondegenerate distribution and the dominant contribution of electron-electron scattering to the hole carrier relaxation processes. These features account for the unusual transport and optical properties of HTS.

In the framework of the proposed model the phase diagram Ln-214 HTS compounds is constructed. The remarkable accord between calculated and experimental phase diagrams may be considered as the confirmation of the supposed model. Thus the HTSs may be considered as the special class of solids in-between insulator and metal where the unusual mechanism of superconductivity resulting from interaction of electron pair with -U centers is realized.

VI. ACKNOWLEDGMENTS

We are grateful for valuable discussions with L. V. Keldysh, B. A. Volkov, E. G. Maksimov and P. A. Arseev.

-
- ¹ J. G. Bednorz and K. A. Müller, Z. Phys. B **64**, 189 (1986).
 - ² V. M. Loktev, Fiz. Nizk. Temp. **22**, 3 (1996) [Low Temp. Phys. **22**, 211 (1996)].
 - ³ P. W. Anderson, Phys. Rev. Lett. **34**, 953 (1975).
 - ⁴ E. Simanek, Solid State Commun. **32**, 731 (1979).
 - ⁵ C. S. Ting, D. N. Talwar, and K. L. Ngai, Phys. Rev. Lett. **45**, 1213 (1980).
 - ⁶ H.-B. Schüttler, M. Jarrell, and D. J. Scalapino, Phys. Rev. Lett. **58**, 1147 (1987).
 - ⁷ J. Yu, S. Massida, A. J. Freeman, and D. D. Koelling, Phys. Lett. A **122**, 203 (1987).
 - ⁸ B. A. Volkov, V. V. Tugushev, Pis'ma Zh. Teor. Fiz. **46**, 193 (1987) [Sov. Phys. - JETP Lett., **46**, 245 (1987)].
 - ⁹ G. M. Eliashberg, Pis'ma Zh. Teor. Fiz. **46** (supplement) 94 (1987) [Sov. Phys. - JETP Lett. **46** (supplement), S81 (1987)].
 - ¹⁰ I. O. Kulik, Fiz. Nizk. Temp. **13** 879 (1987) [Low Temp. Phys. **13** 505 (1987)].
 - ¹¹ J. Zaanen, G. A. ZSawatzky, and J. W. Allen, Phys. Rev. Lett. **55**, 418 (1985).
 - ¹² Y. Ohta, T. Tohyama, and S. Maekawa, Phys. Rev. Lett. **66**, 1228 (1991).
 - ¹³ S. Mazumdar, Solid State Commun. **69**, 527 (1989).
 - ¹⁴ H. Eschrig, Physica C **159**, 545 (1989).
 - ¹⁵ H. Romberg, M. Alexander, N. Nucker, P. Adelmann, and J. Fink, Phys. Rev. B **42**, 8768 (1990).
 - ¹⁶ R. L. Martin, Phys. Rev. B **53**, 15501 (1996).
 - ¹⁷ P. C. Hammel, R. L. Martin, B. W. Statt, F. C. Chou, D. C. Johnston, and S.-W. Cheong, Phys. Rev. B **57**, 712 (1998).
 - ¹⁸ D. R. Harshman and A. P. Mills, Jr., Phys. Rev. B **45**, 10684 (1992).
 - ¹⁹ Y. Guo, J. M. Langlois, and W. A. Goddard III, Science **239**, 896 (1988).
 - ²⁰ In $\text{Ba}_{1-x}\text{K}_x\text{BiO}_3$, the -U centers are formed at the neighboring Bi cations if there are three K ions in the eight cells surrounding each of these cations; i.e., each hole lowers $\Delta_{ct} \approx 2$ eV by ~ 0.6 eV. The less pronounced effect of hole in $\text{Ba}_{1-x}\text{K}_x\text{BiO}_3$ as compared to La-214 is accounted for by the fact that the negatively charged (with respect to Ba) K ion is in close vicinity to Bi ion.
 - ²¹ In $\text{Ba}_{1-x}\text{K}_x\text{BiO}_3$, this occurs if there are four K ions in the eight cells that surround a Bi ion.
 - ²² P. G. Radaelli, D. G. Hinks, A. W. Mitchell, B. A. Hunter, J. L. Wagner, B. Dabrowski, K. G. Vandervoort, H. K. Viswanathan, J. D. Jorgensen, Phys. Rev. B **49**, 4163 (1994).
 - ²³ K. Yoshimura, H. Kubota, H. Tanaka, Y. Date, M. Nakanishi, T. Ohmura, N. Saga, T. Sawamura, T. Uemura, K. Kosuge, J. Phys. Soc. Jpn. **62** 1114 (1993).
 - ²⁴ E. F. Paulus, I. Yehia, H. Fuess, J. Rodriguez, T. Vogt, J. Strobel, M. Klauda, G. Saemann-Ischenko, Solid State Commun. **73** 791 (1990).
 - ²⁵ J. M. Ziman. Models of disorder. The theoretical physics of homogeneously disordered systems.-L.-N.Y.-M.: Cambridge University Press, 1979.
 - ²⁶ A. R. Moodenbaugh, Y. Xu, M. Suenaga, T. J. Folkerts, R. N. Shelton, Phys. Rev. B **38**, 4596 (1988).
 - ²⁷ K. Kumagai, K. Kawano, I. Watanabe, K. Nishiyama, K. Nagamine, J. Supercond. **7**, 63 (1994).
 - ²⁸ H. Takagi, S. Uchida, and Y. Tokura, Phys. Rev. Lett. **62**, 1197 (1989).
 - ²⁹ K. Kitazawa, Y. Tomioka, T. Nagano, and K. Kishio, J. Supercond. **7**, 27 (1994).
 - ³⁰ The failure of 2D-percolation over the segments with $L = 3$ in $\text{Nd}_{2-x}\text{Ce}_x\text{CuO}_4$ is also connected with the absence of doped holes conglomerating the singlet hole orbitals of -U centers.
 - ³¹ R. Yoshizaki, N. Ishikawa, H. Sawada, E. Kita, A. Tasaki, Physica C **166**, 417 (1990).
 - ³² C. Marin, T. Charvolin, D. Braithwaite and R. Calemczuk, Physica C **320**, 197 (1999).
 - ³³ Y. Ando, G. S. Boebinger, A. Passner, T. Kimura, K. Kishio, Phys. Rev. Lett. **75**, 4662 (1995).
 - ³⁴ H. Ding, T. Yokoya, J. C. Campuzano, T. Takahashi, M. Randeria, M. R. Norman, T. Mochiku, K. Kadowaki, and J. Giapintzakis, Nature **382**, 51, (1996).
 - ³⁵ S. Marshall, D. S. Dessau, A. G. Loeser, C.-H. Park, A. Y. Matsuura, J. N. Eckstein, I. Bozovic, P. Fournier, A. Kapitulnik, W. E. Spicer, Z. -X. Shen, Phys. Rev. Lett. **76**, 4841 (1996).
 - ³⁶ H. Ding, M. R. Norman, T. Yokoya, T. Takuechi, M. Randeria, J. Campuzano, T. Takahashi, T. Mochiku, and K. Kadowaki, Phys. Rev. Lett. **78**, 2628 (1997).
 - ³⁷ O. M. Ivanenko and K. V. Mitsen, Physica C **235-240**, 2361 (1994).
 - ³⁸ W. A. Little, Phys. Rev. **134**, A1416 (1964).
 - ³⁹ V. L. Ginsburg, Zh. Eksp. Teor. Fiz. **47**, 2318 (1964) [Sov. Phys. - JETP **20**, 1549 (1965)].
 - ⁴⁰ C. M. Varma, P. B. Littlewood, S. Schmitt-Rink, E. Abrahams and A. E. Ruckenstein, Phys. Rev. Lett. **63**, 1996 (1989).
 - ⁴¹ A. Kapitulnik, Physica C **153-155**, 520 (1988).
 - ⁴² N. G. Ong, T. W. Jing, T. R. Chien, Z. Z. Wang, T. V. Ramakrishnan, J. M. Tarascon, and K. Remschnig, Physica C **185-189**, 34 (1991).
 - ⁴³ A. H. MacDonald, Phys. Rev. Lett. **44**, 489 (1980).
 - ⁴⁴ J. C. Garland and R. Bowers, Phys. Rev. Lett. **21**, 1007 (1968).
 - ⁴⁵ M. Gurvitch, A. K. Ghosh, B. L. Gyorffy, H. Lutz, O. F. Kammerer, J. S. Rosner, and M. Strongin, Phys. Rev. Lett. **41**, 1616 (1978).
 - ⁴⁶ Z. Schlesinger, R. T. Collins, F. Holtzberg, C. Feild, G. Koren, A. Gupta, Phys. Rev. B **41**, 11237 (1990).
 - ⁴⁷ D. B. Tanner, M. A. Quijada, D. N. Basov, T. Timusk, R. J. Kelley, M. Onellion, B. Dabrowski, J. P. Rice, D. M. Ginsberg, J. Supercond. **8**, 563 (1995).

FIG. 1. (a) Electron spectrum of charge-transfer insulator in the vicinity of E_F ; (b) Modification of electron spectrum of a charge-transfer insulator as a result of doping (1 - the pair level of -U center).

FIG. 2. Four significant variants of relative positions of the nearest dopant ion projections. Here, the fragments of crystal structure are on the left, and the corresponding projections onto the CuO_2 plane are on the right. Ions of Sr (Ba, Ce) can also reside on opposite sides of the CuO_2 plane. In $\text{Nd}_{2-x}\text{Ce}_x\text{CuO}_4$, there are no apical oxygen ions. 1 - -U centers, 2 - localization areas for doped carriers, 3 - Cu ion, for that Δ_{ct} vanishes for one-electron transitions. (a, b) Two types of $\text{M}_2\text{Cu}_2\text{O}_n$ clusters that form the -U centers at the interior Cu ions in CuO_2 plane (for Ln-214, M=Cu in the self-same CuO_2 plane); (a) $L = 3a$, (b) $L = a\sqrt{5}$. (c) $L = a\sqrt{8}$. This relative position of the nearest projections of dopant ions corresponds to insulator. (d) $L = 2a$. This is an $\text{M}_2\text{Cu}_2\text{O}_n$ cluster serving as a nucleus of normal phase.

FIG. 3. The area of the doped hole localization in the CuO_2 plane (shaded) involves 12 oxygen ions. Here, crosses are copper ions, open circles are oxygen ions, and solid squares are Cu ions for which Δ_{ct} is depressed by 1.8 eV owing to the presence of a hole at three neighboring oxygen ions.

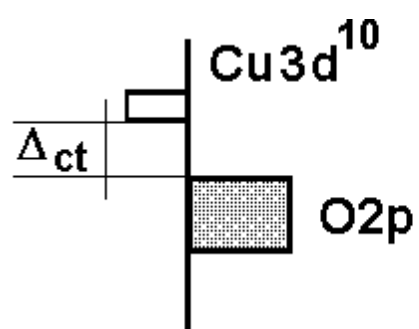
FIG. 4. Formation of bonding orbital (shaded) of a singlet hole pair of -U center from $\pi p_{x,y}$ oxygen orbitals.

FIG. 5. Constructions illustrating the method for determining the percolation threshold for segments with a length of $L = \sqrt{5}$ in a square lattice. (a) Correct determination of the percolation threshold for segments with length $L = \sqrt{5}$ in the case where the distance between atoms is no less than L ; (b) Determination of the percolation threshold for $L = \sqrt{5}$ if there are segments with $L = 2$ yields an underestimated value of x_p because of overlapping of the circles. The segments with $L = 2$ are shown by triple lines. The areas corresponding to superposition of the circles are shaded.

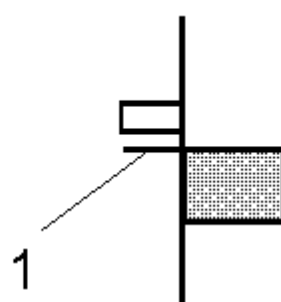
FIG. 6. (a) Boundaries of the percolation regions for the segments with various values of L . The left side of each rectangle corresponds to the 2D-percolation threshold for the segments with length L (under the condition of random distribution of the circles with radius of $L/2$ over the sites and of the absence of the segments with the length smaller than L). The right side of a rectangle is related to the point of the largest number of segments with the length L and corresponds to the ordered arrangement of atoms in a square lattice with cell size L . The corresponding value of L^2 is indicated to the left of each rectangle. An increase in the height of rectangles represents qualitatively an increase in the number of segments with decreasing L . (b - d) Phase diagrams $T_c(x)$ for Ln-214 HTSs. The compositions for which superconductivity was not observed down to 4.2 K are shown by triangles. (b) $\text{La}_{2-x}\text{Ba}_x\text{CuO}_4$;²⁶ (c) $\text{La}_{2-x}\text{Sr}_x\text{CuO}_4$;²⁷ (d) $\text{Nd}_{2-x}\text{Ce}_x\text{CuO}_4$.²⁸

TABLE I. Lower and upper bounds of concentration for percolation over segments with various L . In the rightmost column, it is indicated which state (insulator, ordinary metal, or HTS) would correspond to a given value of L in the case of percolation over the segments with a given L .

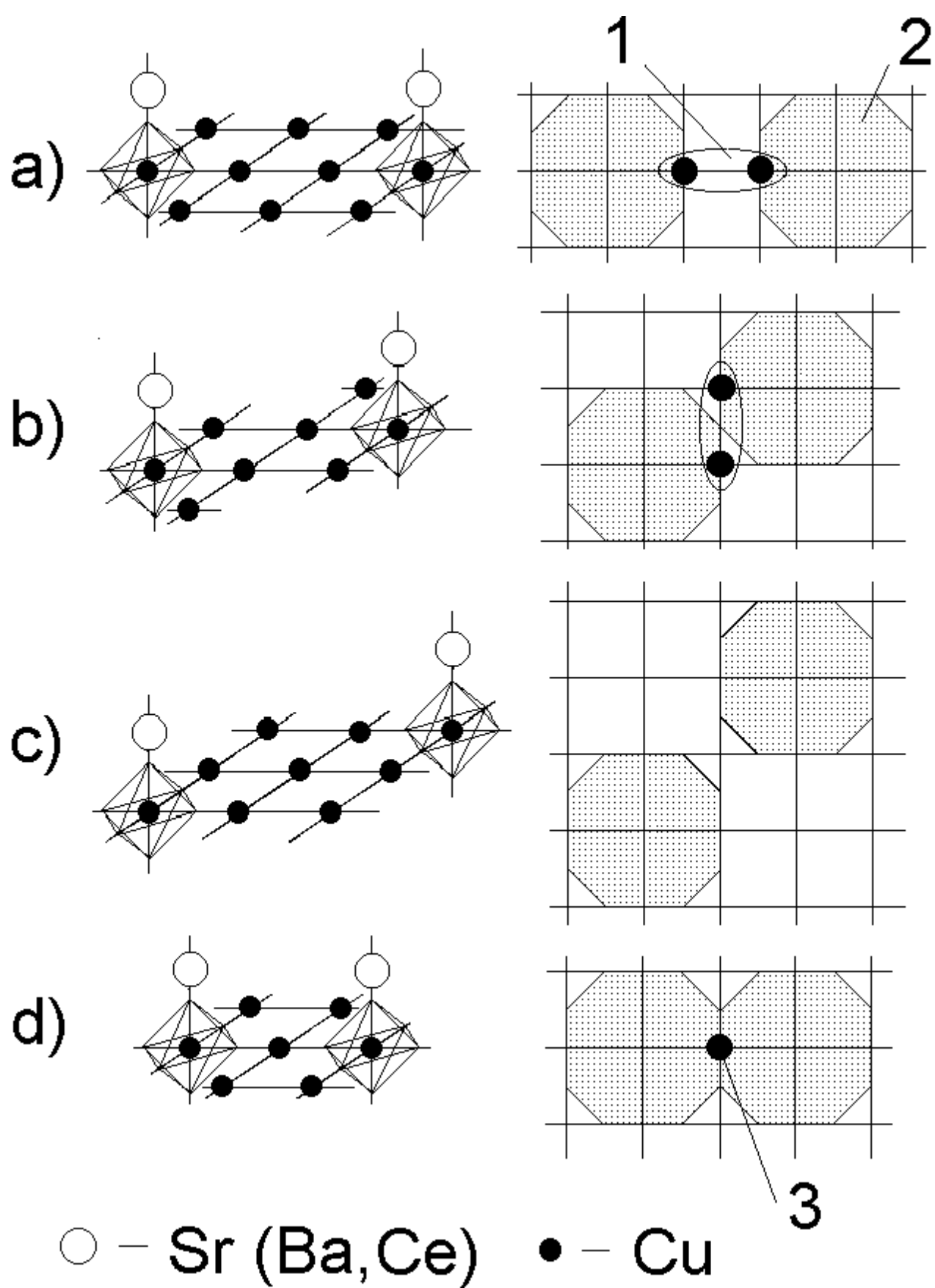
L^2	x_p	x_M	Comments
16	0.0371	0.0625	insulator
13	0.0456	0.0769	insulator
10	0.0593	0.100	insulator
9	0.0659	0.111	HTS
8	0.0742	0.125	insulator
5	0.118	0.200	HTS
4	0.148	0.250	metal

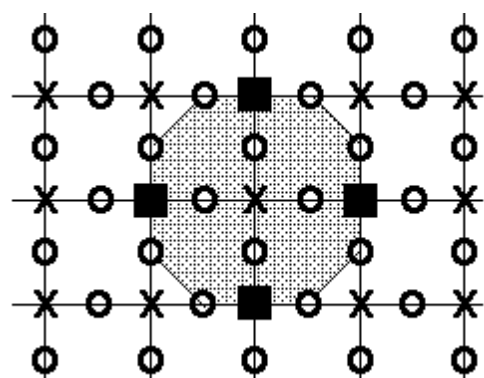


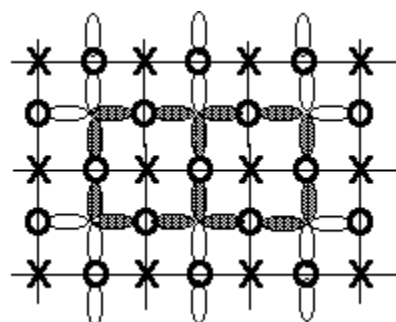
a)

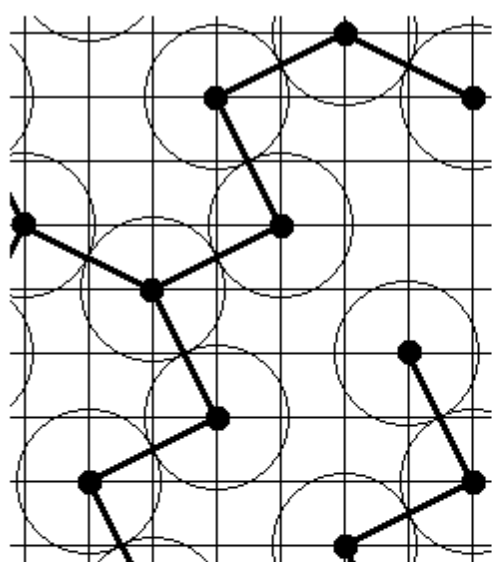


b)

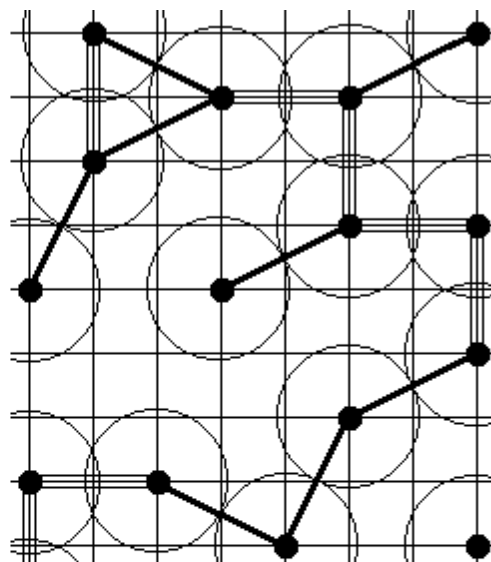








(a)



(b)

